Volume 17, Number 4, 2024. pp. 469-481

Jordan Journal of Physics

ARTICLE

Two–Dimensional Electron-Hole GaAs System in the Static Fluctuation Approximation

Mohamed K. Al-Sugheir[a], **Heba J. Alasali**[b], **Mouath G. Shatnawi**[a] and **Ghassan A. Alnawashi**[a]

[a] *Department of Physics, Faculty of Science, The Hashemite University, 13115, Zarqa, Jordan.*

[b] *Department of Physics, Science Faculty, Isra University, 11622, Amman, Jordan.*

Doi: **https://doi.org/10.47011/17.4.10**

Received on: 30/03/2023; *Accepted on: 26/04/2023*

Abstract: The energy spectrum, particle distribution, internal energy, and specific heat capacity of a two-dimensional electron-hole GaAs system were investigated within the framework of the static fluctuation approximation. The study explored the influence of temperature, dielectric thickness, and dielectric constant on these properties. It was found that the interaction potential had a more pronounced effect on the energy spectrum and distribution of holes than on those of electrons. The results also revealed that the interaction potential effect on internal energy and specific heat capacity of the system occurs at temperatures less than the Fermi temperature. Additionally, the study found that at low temperatures, the system exists in a bound state, whereas at high temperatures, it transitions to a scattering state.

Keywords: Static fluctuation approximation, Two-dimensional electron-hole GaAs system, Energy spectrum, Particle distribution, Heat capacity.

PACS: 65.40. Ba, 71.10. Ca, 71.35. Ee, 73.63.Hs.

1. Introduction

A two-dimensional electron-hole system is a fascinating model with controllable interactions, comprising two parallel layers separated by a distance [1-9]. One layer contains electrons and the other contains holes. The energy spectrum of this system shows that it behaves like an ideal gas if transitions to higher energy states are ignored [1]. The system also exhibits superconductivity due to the pairing of electrons and holes [2]. This system can be analyzed by applying an electric field to double quantum wells [3, 6]. The phases of this system were studied using variational wave functions [9].

Examples of two-dimensional systems are two graphene layers [5, 10, 11], two-dimensional semiconductors [12, 13] and coupled quantum wells [5, 14, 15]. Graphene bilayers can exhibit a Kosterlitz-Thouless temperature as high as room temperature if they have a high number density ($> 10^{13}$ cm^{-2}) and a small interlayer distance (< 2nm) [10]. This indicates that some of these systems can be superfluid near room temperature. This is also possible for double trilayer and quadlayer graphene sheets [11]. Theoretically, the dielectric function of electron-hole plasma was derived using random phase approximation [12]. The exciton energy states in coupled quantum wells were studied by solving the Schrodinger equation for the GaAs/AlGaAs system [15]. The results showed that the Coulomb correlations can create a degenerate

Corresponding Author: Mohamed K. Al-Sugheir **Email**: msugh@hu.edu.jo

electron-hole liquid when the average distance between the particles is smaller than the size of the exciton [14]. The exchange interaction between electrons and holes was found to be the major barrier for generating entangled photon pairs in semiconductor quantum dots [13].

A two-dimensional electron-hole system is a remarkable system that shows various phenomena such as electron-hole plasma [16], phase transitions from exciton gas to electron-hole plasma [17], and exciton condensate in semiconductor quantum well [18]. Due to its extraordinary behavior, this system has drawn significant research interest over the decades leading to the discovery of many applications [9-18].

A two-dimensional electron-hole system is a useful model for many real systems such as coupled quantum wells and graphene layers [6, 19-23]. One of the interesting phases in this system is the Mott insulator [17], where the system remains insulating despite having a band structure that allows conduction. The phase transition from Mott insulator to electron-hole plasma was studied in quasi-equilibrium [17]. The experimental analysis of the phase diagram of indirect excitons for GaAs/AlGaAs showed that unbound electron-hole plasma appears when the temperature of the system increases [20].

The two-dimensional electron-hole system was studied using the mean field approximation [5, 18]. The results showed that the phase transition is affected by the interlayer interaction and the number density of the system. The SFA is an approximation that can account for the quantum fluctuations that are ignored in the mean field approximation. These fluctuations are more important in low-dimensional systems. While much prior work has focused on the system's electric and magnetic properties, we were specifically interested in studying the thermodynamic properties of the two-dimensional electron-hole system, an area with limited research.

In this work, the macroscopic properties of the two-dimensional electron-hole system are derived from its microscopic properties. This can be done in the framework of the SFA. The SFA was used for various systems ranging from weak to strong interactions [24-34], such as the two-dimensional Ising model [25], liquid helium-4 [24], liquid helium-3 [26], and ^{3}He-HeII [27].

2. Basics of Static Fluctuation Approximation.

The main idea of the SFA is to replace the square of the local field operator with its mean value [24]. This means that the true quantum mechanical spectrum of this operator is replaced with a distribution around its mean value [24-26].

The SFA is used to investigate how the interaction potential parameters, number density, and temperature affect the system's thermodynamic properties, including occupation number, energy spectrum, total energy of the system, and specific heat capacity. These properties depend on the temperature, number density, dielectric interlayer thickness, and dielectric constant of the system. The SFA is applied for the first time to electron-hole systems. For that, a symmetric case is considered in this work, where the electrons and holes have the same number density. This symmetry simplifies the Hamiltonian, as the asymmetric case requires additional terms to account for imbalanced densities between electrons and holes.

According to the main assumption of the SFA, the Hamiltonian $\widehat{H}$ can be expressed as a linear combination of the local field operator $\hat{E}_{k,\sigma}$ and the number of particles operator $\hat{n}_{k,\sigma} = \hat{c}^{+}_{\boldsymbol{k},\sigma}\hat{c}_{\boldsymbol{k},\sigma}$ [24, 26],

$$\widehat{H} = \sum_{\boldsymbol{k},\sigma} \hat{E}_{k,\sigma}\hat{c}^{+}_{\boldsymbol{k},\sigma}\hat{c}_{\boldsymbol{k},\sigma}, \tag{1}$$

where $\hat{c}^{+}_{\boldsymbol{k},\sigma}$ and $\hat{c}_{\boldsymbol{k},\sigma}$ are the creation and annihilation operators of electrons and holes. Here, σ refers to the particle type and k is the wave number of a specific state.

The Heisenberg representation of the creation operator $\hat{c}^{+}_{k,\sigma}(\tau)$ is given by:

$$\hat{c}^{+}_{k,\sigma}(\tau) = \exp(\tau\widehat{H})\hat{c}^{+}_{k,\sigma}(0)\exp(-\tau\widehat{H}), \tag{2}$$

where $\tau \equiv it$. The creation operator in Heisenberg picture obeys the equation of motion:

$$\frac{d\hat{c}^{+}_{k,\sigma}(\tau)}{d\tau} = \left[\widehat{H}, \hat{c}^{+}_{\boldsymbol{k},\sigma}(\tau)\right], \tag{3}$$

where $\tau = it$. The creation and annihilation operators for Fermi system have the following anticommutation relations:

$$\left\{\hat{c}^{+}_{\boldsymbol{k},\sigma}, \hat{c}_{\boldsymbol{p},\sigma_1}\right\} = \delta_{\boldsymbol{k},\boldsymbol{p}}\delta_{\sigma,\sigma_1} \tag{4a}$$

$$\{\hat{c}_{\boldsymbol{p},\sigma}, \hat{c}_{\boldsymbol{q},\sigma_1}\} = 0. \quad (4b)$$

In the SFA, the local field operator is assumed to be Hermitian and commutes with the creation and annihilation operators [24-26]. Based on this assumption and using Eqs. (1)-(4), we can express the local field operator as [26]

$$\hat{E}_{k,\sigma} = \{\hat{c}_{\boldsymbol{k},\sigma}, [\hat{H}, \hat{c}^{+}_{\boldsymbol{k},\sigma}(\tau)]\}. \quad (5)$$

The grand Hamiltonian describing the two-dimensional electron-hole system in second quantization can be written as [5]:

$$\hat{H} = \sum_{k,\sigma}(\varepsilon_\sigma(k) - \mu_\sigma)\hat{c}^{+}_{k,\sigma}\hat{c}_{k,\sigma} + \sum_{k,q,p} V(k)\hat{c}^{+}_{k-q,h}\hat{c}_{k-p,h}\hat{c}^{+}_{q,e}\hat{c}_{p,e}, \quad (6)$$

where $\varepsilon_\sigma(k) = \frac{\hbar^2 k^2}{2m^*_\sigma}$ is the single particle energy, h is Planck's constant ($\hbar = h/2\pi$ Dirac's constant) and m^*_σ is the effective mass of either the electron or hole. μ_e (μ_h) is the chemical potential of the electron (hole) system. $V(k)$ in Eq. (6) is the attractive electron-hole interaction defined by the two-dimensional Fourier image of the screened electron-hole attraction [5, 35, 36]:

$$V(k) = -\frac{\bar{U}\, exp(-kd)}{k + 2(a_e^{-1} + a_h^{-1}) + 4(1 - exp(-2kD))/(ka_e a_h)}. \quad (7)$$

Here, d is the dielectric interlayer thickness, $\bar{U} = Ke^2 n/2\varepsilon$ is the potential strength, K is Coulomb's constant, e is the electronic charge, n is the electron and hole number density, and ε is the dielectric constant of the system, $a_{e,h} = \frac{\hbar^2 \varepsilon}{Ke^2 m^*_{e,h}}$, where m^*_e and m^*_h are the effective masses of electron and hole, respectively. The electron-electron and hole-hole interactions are included in the effective mass in the kinetic energy term based on the effective mass approximation. Also, the spin of electrons and holes is neglected here because we are not interested in magnetization effects [5]. For a neutral electron-hole system, the densities of electrons and holes should be equal.

The grand local field operators of electrons and holes are determined from Eq. (5) and Eq. (6):

$$\hat{E}_{\boldsymbol{k},e} = \varepsilon_e(k) - \mu_e + \sum_q V(|q-k|)\hat{n}_{q,h} \quad (8)$$

and

$$\hat{E}_{\boldsymbol{k},h} = \varepsilon_h(k) - \mu_h + \sum_q V(|q-k|)\hat{n}_{q,e}. \quad (9)$$

In the SFA, the quadratic fluctuations in the local field operator are replaced by their mean value [24, 26]. The true quantum energy spectrum is replaced with a distribution around the mean value of the local field operator:

$$\Delta\hat{E}^2_{k,\sigma} = <\Delta\hat{E}^2_{k,\sigma}> = \phi^2_{k,\sigma} \quad (10)$$

The so-called long-range equation of Fermi system was derived [26]:

$$\langle\hat{n}_{k,\sigma}\hat{A}\rangle = \eta_{0,\sigma}(k)\langle\hat{A}\rangle + \eta_{1,\sigma}(k)\langle\Delta\hat{E}_{k,\sigma}\hat{A}\rangle, \quad (11)$$

where $\hat{A}$ is an arbitrary operator that commutes with the creation and annihilation operators. The functions $\eta_{0,\sigma}(k)$ and $\eta_{1,\sigma}(k)$ are given by [25]:

$$\eta_{0,\sigma}(k) = \frac{1}{2}\left\{\frac{1}{exp[\beta(\langle\hat{E}_{k,\sigma}\rangle + \phi_{k,\sigma})]+1} + \frac{1}{exp[\beta(\langle\hat{E}_{k,\sigma}\rangle - \phi_{k,\sigma})]+1}\right\} \quad (12)$$

$$\eta_{1,\sigma}(k) = \frac{1}{2\phi_{k,\sigma}}\left\{\frac{1}{exp[\beta(\langle\hat{E}_{k,\sigma}\rangle + \phi_{k,\sigma})]+1} - \frac{1}{exp[\beta(\langle\hat{E}_{k,\sigma}\rangle - \phi_{k,\sigma})]+1}\right\}, \quad (13)$$

where the parameter $\beta = \frac{1}{k_B T}$, with k_B being the Boltzmann's constant and T absolute temperature [37]. The long-range equation is a generator equation.

Choosing $\hat{A} = 1$, in Eq. (11) the particle distribution is obtained:

$$\langle\hat{n}_{k,\sigma}\rangle = \eta_{0,\sigma}(k) + \eta_{1,\sigma}(k)\langle\Delta\hat{E}_{k,\sigma}\rangle. \quad (14)$$

Due to the symmetry in the fluctuations of $\Delta\hat{E}_{k,\sigma}$, the mean value $\langle\Delta\hat{E}_{k,\sigma}\rangle$ vanishes. Therefore, the particle distribution becomes

$$\langle\hat{n}_{k,\sigma}\rangle = \eta_{0,\sigma}(k). \quad (15)$$

It is more convenient to rewrite Eq. (11) in terms of the deviations of the occupation-number operator:

$$<\Delta\hat{n}_{k,\sigma}\hat{A}> = \eta_{1,\sigma}(k) <\Delta\hat{E}_{k,\sigma}\hat{A}>. \quad (16)$$

Now, it is possible to obtain the close set of coupled nonlinear integral equations. Choosing $\hat{A} = \Delta\hat{E}_{k,\sigma}$ in Eq. (16), we obtain the quadratic fluctuations in the grand local field operator $\Delta\hat{E}^2_{k,\sigma}$:

$$\eta_{1,\sigma}(k)\phi^2_{k,\sigma} = <\Delta\hat{n}_{k,\sigma}\Delta\hat{E}_{k,\sigma}>. \quad (17)$$

Using Eqs. (8), (9), and (17), the quadratic fluctuations in the grand local field operator for electrons and holes can be written as:

$$\eta_{1,e}(k)\phi_{k,e}^2 = \sum_{\boldsymbol{q}} V(|\boldsymbol{q}-\boldsymbol{k}| < \Delta\hat{n}_{k,e}\Delta\hat{n}_{\boldsymbol{q},h} >, \quad (18)$$

$$\eta_{1,h}(k)\phi_{k,h}^2 = \sum_{\boldsymbol{q}} V(|\boldsymbol{q}-\boldsymbol{k}| < \Delta\hat{n}_{k,h}\Delta\hat{n}_{q,e} >. \quad (19)$$

Choosing $\sigma \equiv e$ in Eq. (16) to refer to electrons and using $\hat{A} = \Delta\hat{n}_{q,h}$, we get the pair correlation function $< \Delta\hat{n}_{k,e}\Delta\hat{n}_{q,h} >$,

$$\begin{aligned} < \Delta\hat{n}_{k,e}\Delta\hat{n}_{q,h} > &= \eta_{1,e}(k) < \Delta\hat{E}_{k,e}\Delta\hat{n}_{q,h} > \\ &= \eta_{1,e}(k)\sum_{\boldsymbol{p}} V(|\boldsymbol{k}-\boldsymbol{p}|) < \Delta\hat{n}_{p,h}\Delta\hat{n}_{q,h} >. \\ &= \eta_{1,e}(k)\sum_{\boldsymbol{p}} V(|\boldsymbol{k}-\boldsymbol{p}|)\,(\langle\Delta\hat{n}_{p,h}{}^2\rangle\delta_{p,q} + < \\ &\Delta\hat{n}_{p,h}\Delta\hat{n}_{q,h} >_c) \end{aligned} \quad (20)$$

Choosing $\sigma \equiv e$ in Eq. (16) and $\hat{A} = \Delta\hat{n}_{q,e}$, where $q \neq k$ we get the pair correlation function $< \Delta\hat{n}_{k,e}\Delta\hat{n}_{q,e} >_c$, the index c denoting the true correlation function $q \neq k$.

$$\begin{aligned} < \Delta\hat{n}_{k,e}\Delta\hat{n}_{q,e} >_c &= \eta_{1,e}(k) < \Delta\hat{E}_{k,e}\Delta\hat{n}_{q,e} > \\ &= \eta_{1,e}(k)\sum_{p} V(|k-p|) < \Delta\hat{n}_{p,h}\Delta\hat{n}_{q,e} >. \end{aligned} \quad (21)$$

Choosing $\sigma \equiv h$ in Eq. (16) and $\hat{A} = \Delta\hat{n}_{q,h}$, where $q \neq k$ we get the pair correlation function $< \Delta\hat{n}_{k,h}\Delta\hat{n}_{q,h} >_c$.

$$\begin{aligned} < \Delta\hat{n}_{k,h}\Delta\hat{n}_{q,h} >_c &= \eta_{1,h}(k) < \Delta\hat{E}_{k,h}\Delta\hat{n}_{q,h} > \\ &= \eta_{1,h}(k)\sum_{\boldsymbol{p}} V(|\boldsymbol{k}-\boldsymbol{p}|) < \Delta\hat{n}_{p,e}\Delta\hat{n}_{q,h} >. \end{aligned} \quad (22)$$

The closed system of coupled nonlinear integral equations consisting of $\langle\hat{E}_{k,e}\rangle$, $\langle\hat{E}_{k,h}\rangle$, $\langle\hat{n}_{k,e}\rangle$, $\langle\hat{n}_{k,h}\rangle$, $\phi_{k,e}$, $\phi_{k,h}$, $\langle\Delta\hat{n}_{p,e}\Delta\hat{n}_{q,h}\rangle$, $< \Delta\hat{n}_{k,h}\Delta\hat{n}_{q,h} >_c$ and $< \Delta\hat{n}_{k,e}\Delta\hat{n}_{q,e} >_c$ can be solved numerically by Gaussian quadrature point method [25, 38]. The energy in our calculations is in units of eV.

3. Results and Discussion

In this work, the effect of temperature T, dielectric thickness d, and dielectric constant ε on the distribution and energy spectrum of electrons and holes, internal energy, and specific heat capacity of the GaAs system were examined. Although the effective masses of electrons (m_e^*) and holes (m_h^*) are T-dependent, for convenience we assumed them to be constant across the examined temperature range of 1–50 K. Here, we used $m_h^* = 0.45m_e$ and $m_e^* = 0.067m_e$ [39, 40], where m_e is the electron mass. In temperatures below 150 K, the effective mass of the electron remains nearly constant, close to $m_e^* = 0.067m_e$ [41].

The distribution of electrons and holes at various temperatures is shown in Figs. 1 and 2, respectively. At T = 1 K, both distributions display a step-like behavior, with a high occupation probability (≈ 1) for states below the Fermi momentum k_f. The Fermi temperatures of electrons and holes are 41.5 and 6.2 K, respectively. At T = 1 K, all holes are in the ground state with $k < k_f$. As the temperature increases to be greater than the Fermi temperature, some particles are excited to states above the Fermi level. This depletion from the ground state to excited states increases as the temperature increases. At T = 25 K, the probability of occupying the zero-momentum state is approximately 0.88 for electrons and 0.49 for holes, situating this temperature below the Fermi temperature for electrons but above that for holes. By T = 50 K, most holes are in higher energy states, reflecting their excitation above the Fermi temperature, while electrons still predominantly occupy lower energy states due to their higher Fermi temperature.

The energy spectrum for electrons and holes is the expectation value of the local field operator which is given by

$$\langle\hat{E}_{\boldsymbol{k},e}\rangle = \varepsilon_e(k) + \sum_q V(|q+k|)\langle\hat{n}_{q,h}\rangle, \quad (23)$$

and

$$\langle\hat{E}_{\boldsymbol{k},h}\rangle = \varepsilon_h(k) + \sum_{\boldsymbol{q}} V(|\boldsymbol{q}+\boldsymbol{k}|)\langle\hat{n}_{q,e}\rangle. \quad (24)$$

Figures 3 and 4 show how the energy spectra of electrons and holes change with temperature. The results indicate that the energy of states below the Fermi level is T-dependent. At high-energy states, $k > k_f$, the kinetic energy term is dominant, while the interaction term significantly influences the low-energy states. The interaction potential is attractive and inversely related to k. The system is bound for $k < k_f$ and in a scattering state for $k > k_f$. The temperature effect in the interaction term comes from the distribution of particles. As temperature rises, more particles are excited to states with $k > k_f$, diminishing the influence of the attractive potential with higher k.

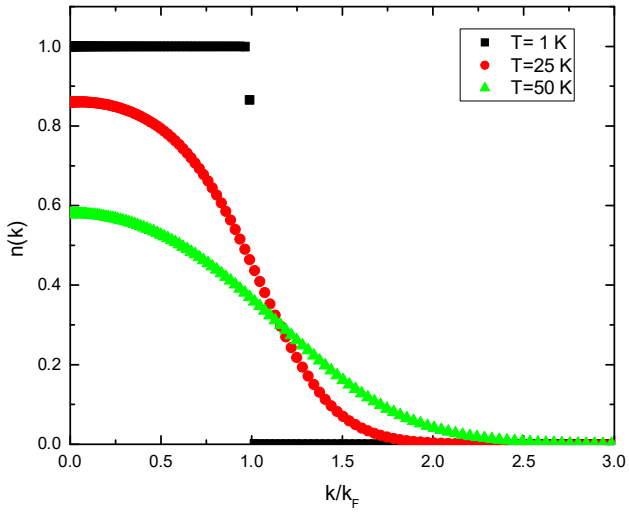

FIG. 1. The electron distribution as a function of k/k_f at values of $\varepsilon = 3$, $d = 5nm$, number density $n = 1x10^{11}\ cm^{-2}$, $m_h^* = 0.45m_e$, and $m_e^* = 0.067m_e$.

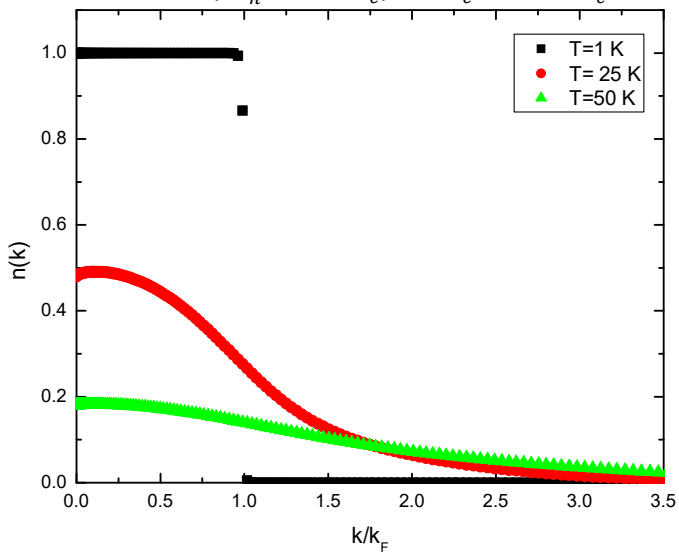

FIG. 2. The hole distribution as a function of k/k_f at values of $\varepsilon = 3$, $d = 5nm$, number density $n = 1x10^{11}\ cm^{-2}$, $m_h^* = 0.45m_e$, and $m_e^* = 0.067m_e$.

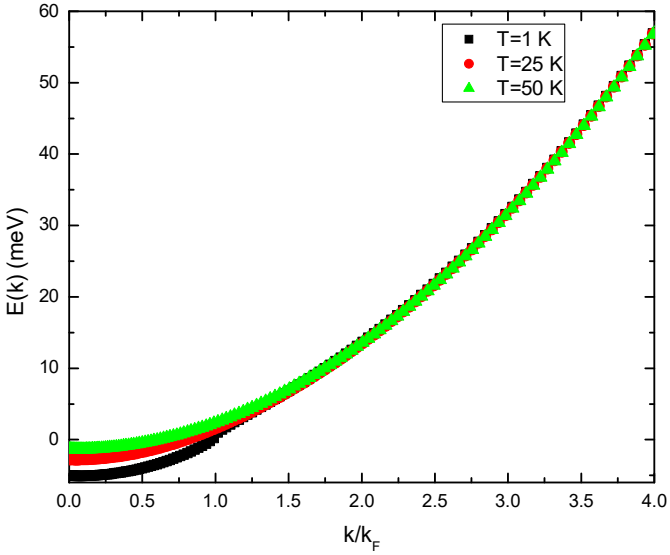

FIG. 3. The electron energy spectrum as a function of k/k_f at values of $\varepsilon = 3$, $d = 5nm$, number density $n = 1x10^{11}\ cm^{-2}$, $m_h^* = 0.45m_e$, and $m_e^* = 0.067m_e$.

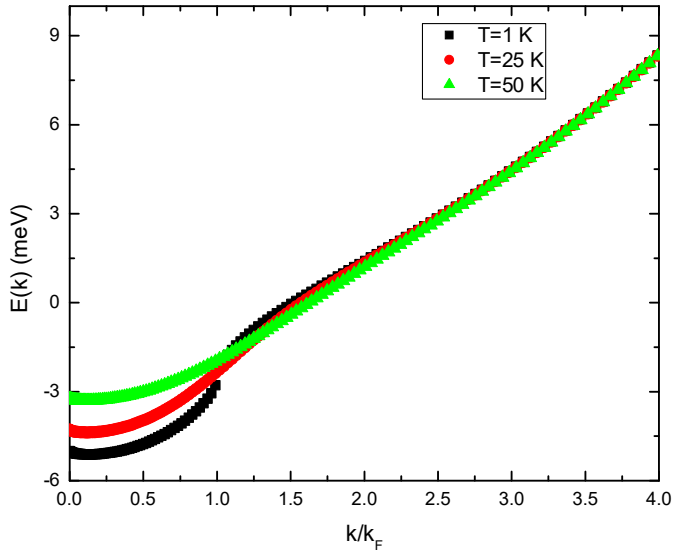

FIG. 4. The hole energy spectrum as a function of k/k_f at values of $\varepsilon = 3$, $d = 5nm$, number density $n = 1x10^{11}\ cm^{-2}$, $m_h^* = 0.45m_e$ and $m_e^* = 0.067m_e$.

The electron and hole distributions at T = 25 K with different dielectric interlayer thicknesses d are shown in Figs. 5 and 6, respectively. Results indicate that the electron distribution is not sensitive to d, while the hole distribution in the lowest states is shifted upward as the dielectric interlayer thickness decreases, where the attractive potential decreases as d increases (the attractive potential is proportional to e^{-kd}). Given that the effective masses of electrons and holes are $0.067m_e$ and $0.45m_e$, respectively, electrons possess higher kinetic energy than holes. Therefore, the attractive potential influences the hole distribution more than the electron distribution.

The energy spectra of electrons and holes at T = 25 K are presented in Figs. 7 and 8, respectively. The results indicate that the energy spectrum of electrons exhibits a parabolic dependence on momentum, where the kinetic energy of the electrons is dominant in the higher energy states. It is only shifted downward as the interaction potential increases (d decreases). The spectrum of the hole energy (Fig. 8) is more influenced by the interaction term in the local field operator, as holes have a greater effective mass than electrons. Therefore, holes in the lowest states become more bound due to the effect of the attractive potential. In both cases, the interaction potential affects mainly the lowest states up to states with momentum comparable to the Fermi momentum.

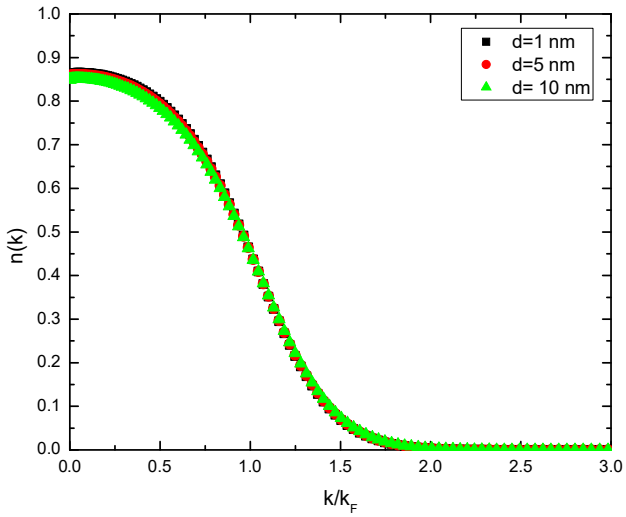

FIG. 5. The electron distribution as a function of k/k_f at values of $T = 25$ K, $\varepsilon = 3$, number density $n = 1x10^{11}\ cm^{-2}$, $m_h^* = 0.45m_e$, and $m_e^* = 0.067m_e$.

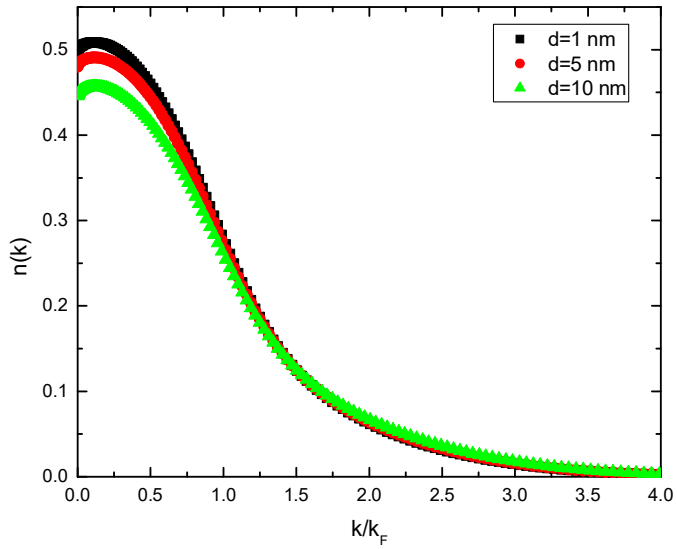

FIG. 6. The hole distribution as a function of k/k_f at values of $T = 25$ K, $\varepsilon = 3$, number density $n = 1x10^{11}\ cm^{-2}$, $m_h^* = 0.45m_e$, and $m_e^* = 0.067m_e$.

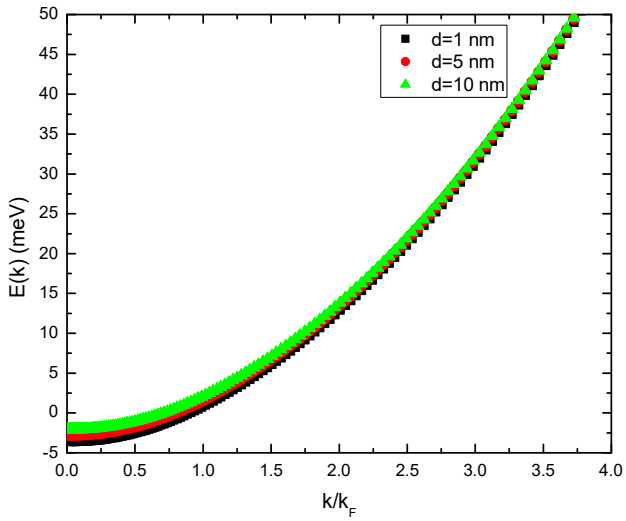

FIG. 7. The electron energy spectrum as a function of k/k_f at values of $T = 25$ K, $\varepsilon = 3$, number density $n = 1x10^{11}\ cm^{-2}$, $m_h^* = 0.45m_e$, and $m_e^* = 0.067m_e$.

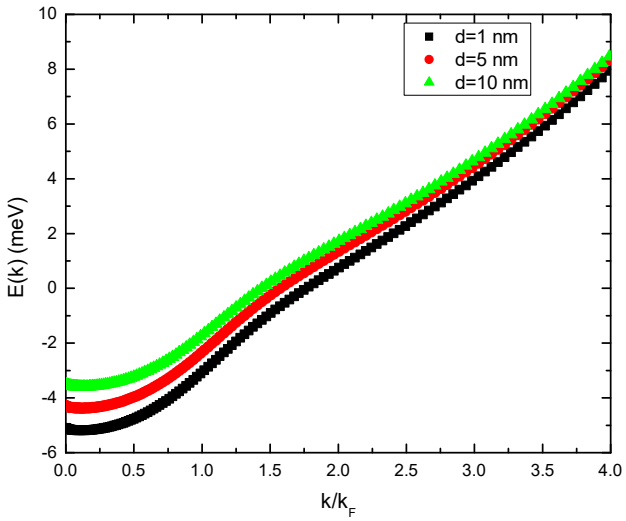

FIG. 8. The hole energy spectrum as a function of k/k_f at values of $T = 25$ K, $\varepsilon = 3$, number density $n = 1x10^{11}\ cm^{-2}$, $m_h^* = 0.45m_e$, and $m_e^* = 0.067m_e$.

The effect of the dielectric constant on the electron and hole distributions is shown in Figs. 9 and 10. The figures show that as the dielectric constant increases, the probability of finding a particle in states with momentum below the Fermi momentum decreases. The pair potential is inversely proportional to the dielectric constant, so the system is more attractive as the dielectric constant decreases. The distribution of holes is more sensitive to the dielectric constant than that of electrons, as electrons have higher kinetic energy. The results show that the Fermi temperature of the system increases as the dielectric constant decreases, where the probability of having a particle in a state with $k < k_F$ increases as the dielectric constant decreases.

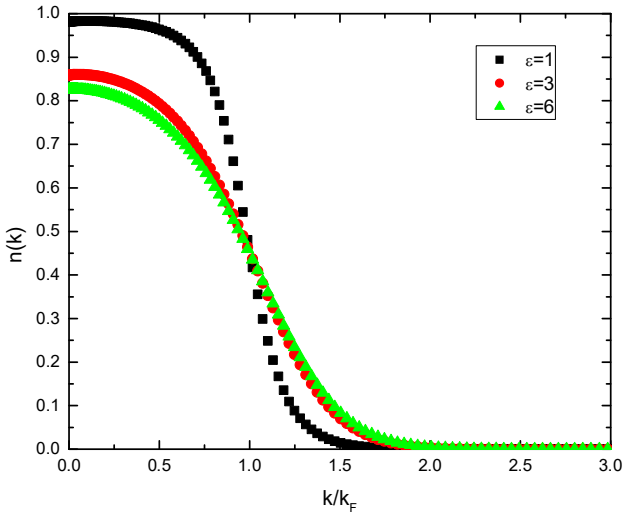

FIG. 9. The electron distribution as a function of k/k_f at values of $T = 25$ K, $d = 5nm$, number density $n = 1x10^{11}\ cm^{-2}$, $m_h^* = 0.45m_e$, and $m_e^* = 0.067m_e$.

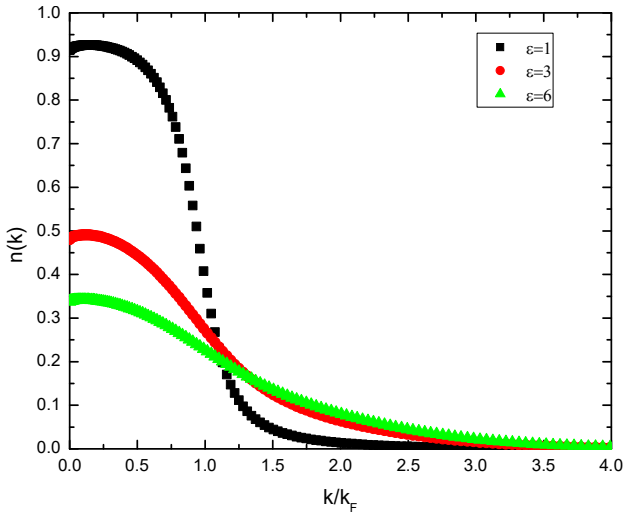

FIG. 10. The hole distribution as a function of k/k_f at values of $T = 25$ K, $d = 5nm$, number density $n = 1x10^{11}\ cm^{-2}$, $m_h^* = 0.45m_e$, and $m_e^* = 0.067m_e$.

Figures 11 and 12 present the energy spectrum of electrons and holes across different dielectric constants. The results indicate that the spectrum of both electrons and holes behaves like a non-interacting system at high momentum states, $k > k_F$, where the kinetic energy is dominant in the local field operator. In low momentum states, $k < k_F$, the energy spectrum is shifted downward with increasing the pair potential (the dielectric constant decreases). This result indicates that the pair potential affects mainly the low-lying energy states, which is proportional to e^{-kd}.

The influence of the interaction potential on the internal energy per particle, $\frac{U}{N}$, and specific heat capacity, $\frac{C_A}{Nk_B}$, is examined. Figure 13 shows how $\frac{U}{N}$ varies with the dielectric interlayer

thickness. $\frac{U}{N}$ has the same behavior for any value of thickness. The interaction potential affects $\frac{U}{N}$ mainly at low temperatures ($T < T_F$, where T_F is the Fermi temperature). As temperature rises, $\frac{U}{N}$ becomes similar across thickness values because the kinetic energy becomes dominant. Figure 14 shows how $\frac{C_A}{Nk_B}$ depends on temperature for different values of the thickness of the dielectric interlayer. The results indicate that $\frac{C_A}{Nk_B}$ increases with T until it reaches a maximum value at $T = T_F$ and then decreases to the classical value of a two-dimensional non-interacting system at high temperatures. The "bump" in $\frac{C_A}{Nk_B}$ suggests an order-disorder transition, shifting from a more ordered low-temperature quantum regime to a less ordered high-temperature classical regime.

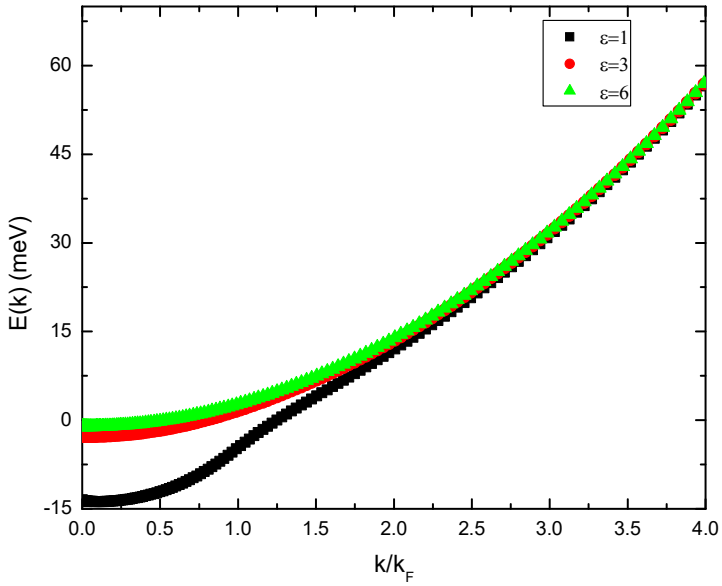

FIG. 11. The energy spectrum of electrons as a function of k/k_f at values of $T = 25$ K, $d = 5nm$, number density $n = 1x10^{11}\ cm^{-2}$, $m_h^* = 0.45m_e$, and $m_e^* = 0.067m_e$.

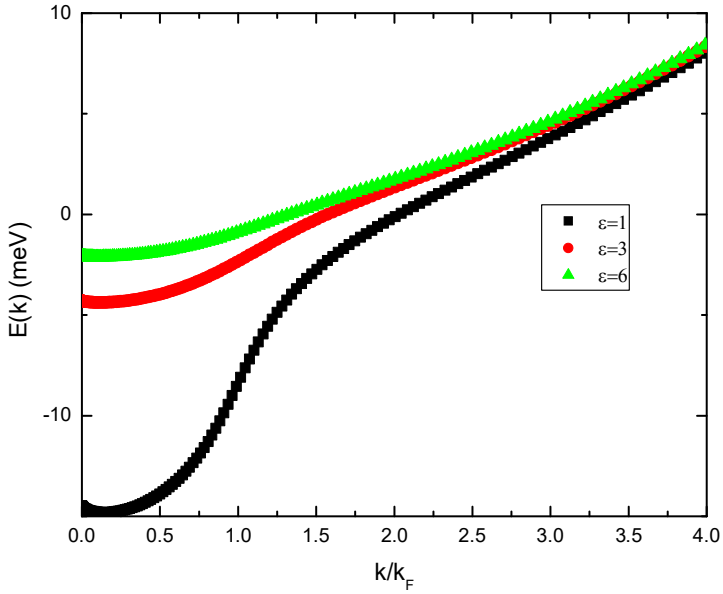

FIG. 12. The hole spectrum as a function of k/k_f at values of $T = 25$ K, $d = 5nm$, number density $n = 1x10^{11}\ cm^{-2}$, $m_h^* = 0.45m_e$, and $m_e^* = 0.067m_e$.

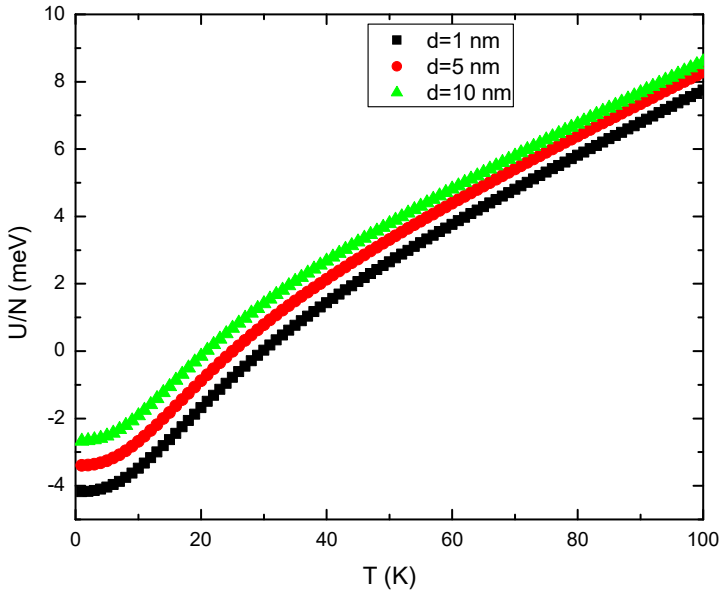

FIG. 13. The energy of the system as a function of temperature at values of $\varepsilon = 3$, number density $n = 1x10^{11}\ cm^{-2}$, $m_h^* = 0.45m_e$, and $m_e^* = 0.067m_e$.

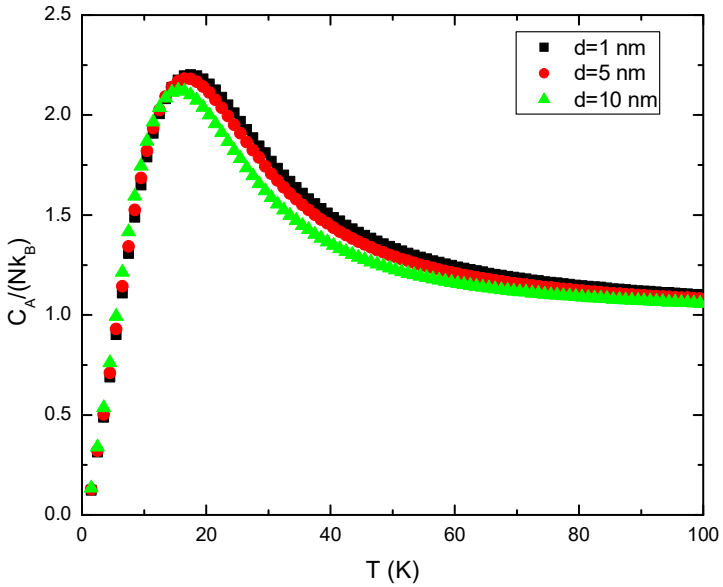

FIG. 14. The specific heat capacity $C_A/(Nk_B)$ as a function of temperature at values of $\varepsilon = 3$, number density $n = 1x10^{11}\ cm^{-2}$, $m_h^* = 0.45m_e$, and $m_e^* = 0.067m_e$

The effect of the dielectric constant on $\frac{U}{N}$ is illustrated in Fig. 15. The results indicate that the interaction potential affects $\frac{U}{N}$ at low temperatures. $\frac{U}{N}$ is negative at low temperatures, where the interaction term in the local field operator becomes dominant. It is well known that as the dielectric constant increases the interaction potential decreases. Therefore, $\frac{U}{N}$ is more negative in the quantum regime (low temperatures) as the dielectric constant decreases. In the classical regime (high temperatures), $\frac{U}{N}$ is slightly dependent on the dielectric constant. Figure 16 shows $\frac{C_A}{Nk_B}$ for different values of the dielectric constant. $\frac{C_A}{Nk_B}$ increases with T until it reaches a maximum value at $T = T_F$. At high temperatures, it approaches the value of a two-dimensional non-interacting system. The results of $\frac{C_A}{Nk_B}$ indicate that the Fermi temperature increases as the interaction increases (dielectric constant decreases).

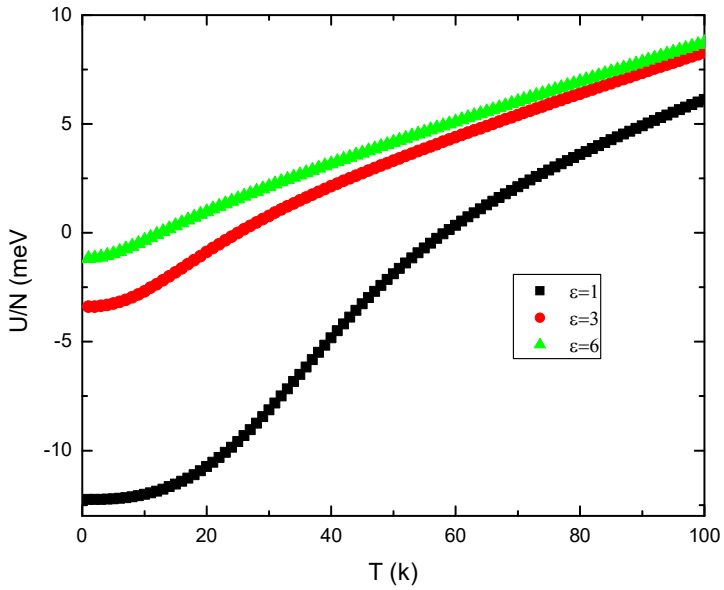

FIG. 15: The energy of the system as a function of temperature at values of $d = 5nm$, number density $n = 1x10^{11}\ cm^{-2}$, $m_h^* = 0.45m_e$, and $m_e^* = 0.067m_e$.

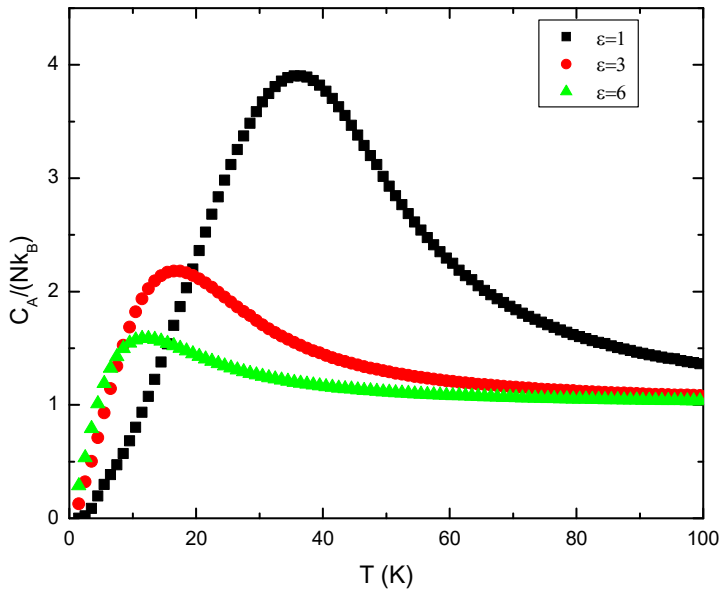

FIG. 16. The specific heat capacity $C_A/(Nk_B)$ as a function of temperature at values of $d = 5nm$, number density $n = 1x10^{11}\ cm^{-2}$, $m_h^* = 0.45m_e$, and $m_e^* = 0.067m_e$.

4. Conclusion

The static fluctuation approximation (SFA) technique was applied successfully to calculate the distribution and energy spectrum of the two-dimensional electron-hole GaAs system. The influence of temperature, dielectric interlayer thickness, and the dielectric constant on these quantities was examined. The results indicate that the interaction term in the local field operator affects these quantities at low-momentum states. The internal energy per particle and specific heat capacity of the GaAs system were also investigated. The system acts like a nearly ideal, non-interacting gas at high temperatures or high momentum. The dielectric constant has a stronger effect on the results than the dielectric interlayer thickness.

The SFA goes well beyond the mean-field approach and has been applied over a wide range of systems ranging from strongly to weakly interacting systems. However, just like other perturbative theories, it is most suitable for weakly interacting or dilute systems. To improve the present framework of the SFA, we could reformulate it to include higher orders of fluctuations.

References

[1] Lerner, I. V. and Lozovik, Y. E., Sov. Phys. JETP, 53 (1981) 763.

[2] Shevchenko, S. I., Phys. Rev. Lett., 72 (1994) 3242.

[3] Yoshioka, D. and MacDonald, A. H., J. Phys. Soc. Jpn., 59 (1990) 4211.

[4] Lai, C. W., Zoch, J., Gossard, A. C., and Chemla, D. S., Science, 303 (2004) 503.

[5] Berman, O. L., Kezerashvili, R. Y., and Ziegler, K., Physica E, 71 (2015) 7.

[6] Kvon, Z. D., Olshanetsky, E. B., Kozlov, D. A., and Dvoretskii, S. A., JETP Lett., 87 (2008) 502.

[7] Huijben, M., Brinkman, A., Koster, G., Rijnders, G., Hilgenkamp, H., and Blank, D.H.A., Adv. Mater., 21 (2009) 1665.

[8] Lozovik, Y. E., Ogarkov, S. L., and Sokolik, A. A., Phys. Rev. B, 86 (2012) 045429.

[9] Tiene, A., Levinsen, J., Parish, M. M., MacDonald, A. H., Keeling, J., and Marchetti, F. M., Phys. Rev. Res., 2 (2020) 023089.

[10] Min, H., Bistrizer, R., Su, J. J., and MacDonald, A. M., Phys. Rev. B, 78 (2008) 121401.

[11] Zarenia, M., Perali, A., Neilson, D., and Peeters, F. M., Sci. Rep., 4 (2014) 7319.

[12] Semkat, D., Stolz, H., Kraeft, W-D., and Fehske, H., J. Phys. Condens. Matter, 33 (2021) 475501.

[13] Kadantsev, E. S. and Hawrylak, P., J. Phys.: Conf. Ser., 248 (2010) 012018.

[14] Babichenko, V. S. and Polishchuk, I. Y., JETP Lett., 97 (2013) 628.

[15] Sivalertporn, K., Phys. Lett. A, 380 (2016) 1990.

[16] Ryzhii, V., Satou, A., and Otsuji, T., J. Appl. Phys., 101 (2007) 024509.

[17] Asano, K. and Yoshioka, T., J. Phys. Soc. Jpn., 83 (2014) 084702.

[18] Zhu, X., Littlewood, P. B., Hybertsen, M. S., and Rice, T. M., Phys. Rev. Lett., 74 (1995) 1633.

[19] Butov, L. V., Zrenner, A., Abstreiter, G., Böhm, G., and Weimann, G., Phys. Rev. Lett., 73 (1994) 304.

[20] Stern, M., Garmider, V., Umansk, V. Y., and Bar-Joseph, I., Phys. Rev. Lett., 100 (2008) 256402.

[21] Lozovik, Y. E. and Sokolik, A. A., JETP Lett., 87 (2008) 55.

[22] Liu, M., Yin, X., and Zhang, X., Nano Lett., 12 (2012) 1482.

[23] Sorianello, V., Midrio, M., and Romagnoli, M., Opt. Expr., 23 (2015) 6478.

[24] Al-Sugheir, M. K., Ghassib, H. B., and Nigmatullin, R. R., Int. J. Theor. Phys., 40 (2001) 1033.

[25] Nigmatullin, R. R., Khamzin, A. A., and Ghassib, H. B., Solid State Commun. 113 (2000) 257.

[26] Al-Sugheir, M. K. and Ghassib, H. B., Int. J. Theor. Phys., 41 (2002) 705.

[27] Al-Sugheir, M. K., Int. J. Theor. Phys., 43 (2004) 1527.

[28] Ghulam, N. M., Ghassib, H. B., and Al-Sugheir, M.K., Phys. Rev. C, 75 (2007) 64317.

[29] Al-Sugheir, M. K., Al-Khzon, H. A., Al-Maghrabi, M., and Alna'washi, G. A., Acta Phys. Pol. A, 122 (2012) 704.

[30] Alhami, E. M., Ghassib, H. B., and Al-Sugheir, M. K., Acta Phys. Pol. A, 127 (2015) 1648.

[31] Al-Khzon, H. and Al-Sugheir, M. K., Eur. Phys. J. B, 94 (2021) 192.

[32] Al-Sugheir, M. K. and Mqbel, F. F., Can. J. Phys., 99 (2021) 841.

[33] Al-Khzon, H. and Al-Sugheir, M. K., Int. J. Mod. Phys. B, 35 (2021) 2150059.

[34] Al-Khzon, H. and Al-Sugheir, M. K., Phys. B, 571 (2019) 18.

[35] Lozovik, Y. E. and Yudson, V. I., Sov. Phys. JETP, 44 (1976) 389.

[36] Lozovik, Y. E. and Yudson, V. I., Sov. Phys. JETP, Lett., 22 (1975) 26.

[37] Feynman, R. P., "Statistical Mechanics", (Benjamin, Reading Massachusetts, 1972).

[38] Burden, R. L. and Faires, J. D., "Numerical Analysis", 5th Ed., (PWS publishing company, Boston, 1993).

[39] Tang, J., Cao, S., Gao, Y., Sun, Y., Geng, W., Williams, D. A., Jin, K., and Xu, X., Appl. Phys. Lett., 105 (2014) 041109.

[40] Hillmer, H., Forchel, A., Hansmann, S., Morohashi, M., and Lopez, E., Phys, Rev. B, 39 (1989) 10901.

[41] Hazama, H., Sugimasa, T., Imachi, T., and Hamaguchi, C., JPSJ, 55 (1986) 1282.